



Cite this: *Chem. Commun.*, 2017, 53, 82

Fluorescent glycoprobes: a sweet addition for improved sensing

Xiao-Peng He,^a Yi Zang,^b Tony D. James,^{*c} Jia Li,^{*b} Guo-Rong Chen^{*a} and Juan Xie^{*d}

The development of small-molecule fluorescent probes for the detection of ions and biomacromolecules and for cellular and *in vivo* imaging has been a very active research area. Nevertheless, many problems exist for traditional probes including their poor water solubility, toxicity and the inability to target specific tissues. Because of the enhanced water solubility, biocompatibility and targeting ability for specific cells, there has been an emerging movement to use carbohydrates as either the backbone or as a warhead to decorate conventional fluorescent probes, producing “glycoprobes” with enhanced properties. This feature article provides an overview of recently developed glycoprobes for ion and protein detection as well as targeted (receptor targeting) cellular imaging and theranostics. Here, we summarise the tactics for preparing small molecular glycoprobes and their supramolecular 2D material composites.

Received 22nd August 2016,
Accepted 3rd October 2016

DOI: 10.1039/c6cc06875h

www.rsc.org/chemcomm

Introduction

The development of fluorescent small-molecular probes is a vibrant research field. Because of their high sensitivity, ease of manipulation and their amenability for analyzing live cells with high resolution, fluorescence techniques have been extensively used for biosensing and bioimaging. Subsequently, many elegant fluorescent sensing mechanisms have been developed and a myriad of molecular probes have been constructed for the detection of ions, small-molecules, and biomacromolecules (such as genes, proteins and saccharides).¹ Many of those probes have shown the potential to be used for cellular imaging as well as *in vivo* tracking of a target species of interest.² However, many problems still exist for the traditional probes which embody hydrophobic organic dyes in terms of the insufficient water solubility, cytotoxicity and the lack of targeting ability for specific types of cells and tissues.

Sugars are naturally existing biomolecules. Besides their role in energy storage and conversion (such as glucose), ligand-type sugars (glycoligands) are also involved in many cell signaling processes through the selective interaction with their receptor

proteins on the cell membrane. The recognition between receptors and glycoligands is responsible for not only physiological events such as cell–cell adhesion, mammalian fertilization and cell differentiation, but also pathological processes including cancer metastasis, virus invasion and bacterial infection.^{3–8} For example, the asialoglycoprotein receptor (ASGPr) that is selectively expressed on hepatocyte has been shown as an invasion site for hepatotropic viruses and overexpressed during liver inflammation.⁹ An upregulation in the expression level of transmembrane mannose receptor was identified for alternatively activated macrophages, facilitating tumorigenesis and tumor metastasis.¹⁰ Influenza viruses also rely on the binding of their surface hemagglutinin to sialyl glycans on host cells as the first crucial step to invasion.¹¹ Given such evidence, the interaction between glycoligands and their receptors has been exploited for targeted delivery of therapeutic agents.^{12,13}

Considering the targeting ability as well as their inherent structural diversity, water solubility and biocompatibility, we sought to incorporate glycoligands into traditional organic-dye based fluorescence probes for enhanced sensing properties. Here we discuss our strategies developed in recent years for the construction of the so-called glycoprobes (glycoligand-based fluorescent probes) and their material composites with low-dimensional materials for targeted imaging and theranostics.

Small-molecular fluorescent glycoprobes for ion and lectin sensing Sugar-ring modified glycoprobes as ion chelators

Sugars are generally water-soluble molecules (except for some polysaccharides in which intermolecular hydrogen bonding

^a Key Laboratory for Advanced Materials & Institute of Fine Chemicals, School of Chemistry and Molecular Engineering, East China University of Science and Technology, 130 Meilong Rd., Shanghai 200237, P. R. China. E-mail: mrs_guorongchen@ecust.edu.cn

^b National Center for Drug Screening, State Key Laboratory of Drug Research, Shanghai Institute of Materia Medica, Chinese Academy of Sciences, 189 Guo Shoujing Rd., Shanghai 201203, P. R. China. E-mail: jli@simm.ac.cn

^c Department of Chemistry, University of Bath, Bath, BA2 7AY, UK. E-mail: t.d.james@bath.ac.uk

^d PPSM, ENS Cachan, CNRS UMR 8531, Université Paris-Saclay, 61 av President Wilson, F-94230 Cachan, France. E-mail: joanne.xie@ppsm.ens-cachan.fr



interactions compromise the solubility) owing to the presence of hydrophilic groups such as hydroxy groups. Moreover, the hydroxy groups on the sugar ring have well-defined orientations. The introduction of a diverse range of pharmacophores to these hydroxy groups has been exploited as an effective strategy for drug discovery.^{14,15} Since the pioneering reports on the use of a monosaccharide as a central scaffold on which fluorophores are installed for ion sensing,^{16,17} a number of these types of glycoprobes incorporating a receptor–sugar–reporter motif have been developed.^{18–30}

Our initial idea of constructing glycoprobes originates from the development of sugar-based enzymatic inhibitors by the

Cu(I)-catalyzed azide–alkyne 1,3-dipolar cycloaddition (CuAAC) click reaction.^{14,15} The 1,4-disubstituted 1,2,3-triazole formed by CuAAC has been demonstrated as a good chelating site for a variety of cations and anions.¹⁵ On the basis of this unique feature of triazole, we sought to graft fluorophores to sugar scaffolds by CuAAC, forming structurally well-defined fluorescence triazolyl glycoprobes for ion sensing. In these glycoprobes, the triazole acts as an ion binder, and the sugar as a rigid scaffold on which fluorophores, the signal reporter, are attached. Both fluorescence “turn-off” and “turn-on” glycoprobes have been developed, based on the different sensing mechanisms involved.



From left to right: Jia Li, Guo-Rong Chen, Yi Zang and Xiao-Peng He

Yi Zang received her PhD in Pharmacology from SIMM (CAS). Following a postdoctoral fellowship at MD Anderson Cancer Center in the US, she returned to SIMM in 2010 as an associate professor. Zang focuses her research on the interactome and identification of novel physiological roles of AMPK, the mechanistic study of cell fate regulation using chemical biology tools, and detection of protein–carbohydrate interactions for disease diagnosis and targeted therapy.

Jia Li received his PhD from SIMM in 2000 and was promoted to professor in 2005. He stayed at University of Cambridge (UK, Feb 2003–Aug 2003) and Garvan Institute of Medical Research (Australia, Aug 2004–Feb 2005) as a visiting scholar. From year 2013 he was appointed as a deputy director of SIMM. Li's research interests are centered on the investigation of mechanisms of metabolic disease for identifying key genetic and biochemical events, chemical biology and high-throughput drug screening. He received the China National Fund for Distinguished Young Scientists in 2011.

Xiao-Peng He received his BS in Applied Chemistry (2006) and PhD in Pharmaceutical Engineering (2011) from ECUST. He conducted a co-tutored doctoral program at ENS Cachan (France) from July 2008 to February 2009 (advisor Prof. Juan Xie) sponsored by the French Embassy. Then he carried out his postdoctoral research with Prof. Kaixian Chen (SIMM, CAS) at ECUST from 2011 to 2013. He's now an associate professor at the Institute of Fine Chemicals, ECUST, where his research interests span chemical glycobiology to construction of fluorescent and electrochemical probes and materials.

Guo-Rong Chen received her BS in Organic Chemical Engineering (1975) from ECUST. She conducted her research at the Glycochemistry Lab of University Lyon 1 from 1989–1991; she revisited the lab in years 1996, 1998 and 2002. Then she spent two years at Shanghai Institute of Materia Medica (CAS) as a visiting scholar. She was appointed as professor at ECUST in 2001. Her research interests involve glycochemistry, medicinal chemistry, chemical glycobiology and green fine chemicals.



Tony D. James

Tony D. James is a Professor at the University of Bath and Fellow of the Royal Society of Chemistry. He obtained his: BSc 1986 (University of East Anglia), PhD 1991 (University of Victoria), and was a Postdoctoral Research Fellow 1991–1995 (with Seiji. Shinkai in Japan). He was a Royal Society Research Fellow from 1995 to 2000 (University of Birmingham). In 2013 he was recognized for his role in developing networks with Japan by the

award of a Daiwa-Adrian Prize and in 2015 he received the Inaugural CASE Prize for establishing and developing networks with China.



Juan Xie

Juan Xie received her PhD in chemistry at University Paris V in 1998 under the supervision of Professors M. C. Fournier-Zaluski and B. P. Roques. After post-doctoral study at CNRS in the group of Dr M. Wakselman, she moved to University Paris VI as an associate Professor (1991). In 2004, she was appointed full Professor at Ecole Normale Supérieure de Cachan. Her current research interest is focused on bio- and photo-active molecules.



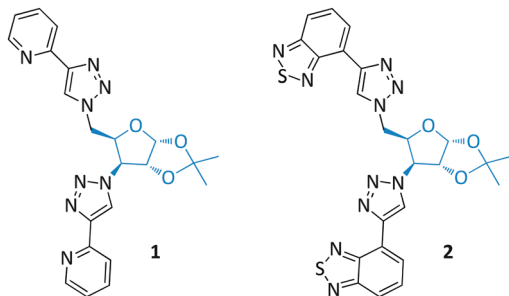


Fig. 1 Structures of glycofuranoside based glycoprobes **1** and **2**.

Two series of glycofuranoside based glycoprobes were synthesized by grafting two-fold chelating groups to a single sugar scaffold using CuAAC (Fig. 1, in cooperation with Policar's group). These intrinsically fluorescent glycoprobes with well-preorganized structures through intermolecular π -interactions were determined to be suitable for metal cation sensing by fluorescence spectroscopy. Both pyridine-grafted (**1**)³¹ and benzothiadiazole-grafted (**2**)³² glycoprobes showed fluorescence quenching in the presence of Cu(II). These types of glycofuranoside based glycoprobes also displayed the ability to penetrate living cell membranes, providing a basis for cell tracking studies.³³

Glucopyranosides, which are a class of structurally more diverse sugars, were also used as the core scaffold for glycoprobe syntheses (Fig. 2). In pursuit of developing novel sugar-based enzymatic inhibitors,³⁴ we synthesized a bis-triazolyl α -ketoester based compound **3**.³⁵ With fluorescence spectroscopy we determined that this compound is fluorescent, and could be used for the fluorescence turn-off detection of Ni(II) over other metal cations. Inspired by this research, we further coupled pyrene to the sugar ring of a glucopyranoside, forming the bis-pyrenyl glycoprobe **4**.³⁶ Interesting, because of the structural rigidity of the sugar scaffold, the pyrene groups on the sugar ring exist predominantly in the excimer form, as determined by fluorescence spectroscopy. This glycoprobe was shown to undergo a selective fluorescence quenching in the presence of Hg(II) over other metal ions.

While these bis-triazolyl glycoprobes demonstrated the possibility of using sugars as a rigid scaffold on which to install fluorophores for ion sensing, several problems exist to limit their realistic applications. On the one hand, the water solubility was reduced due to substitution of the ring hydroxys of the glycosides by the hydrophobic dyes. Therefore, as a result, the detection experiments were performed in organic solvents. Furthermore, the detection mechanism was based on fluorescence quenching, due to the heavy metal effect diminishing the fluorescence

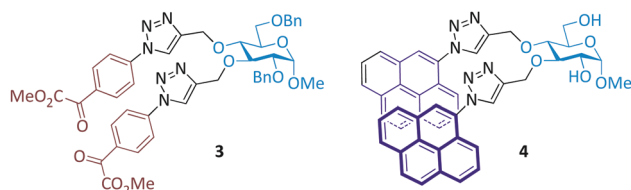


Fig. 2 Structures of glucopyranoside based glycoprobes **3** and **4**.

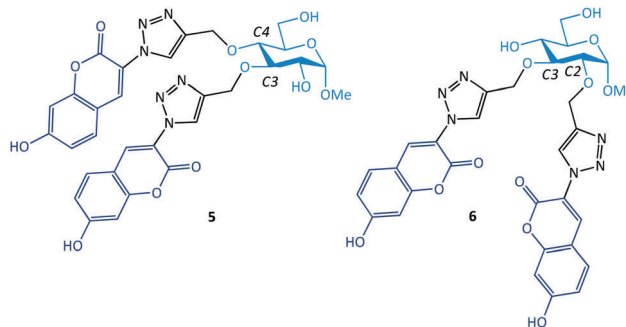


Fig. 3 Structures of glucopyranoside based glycoprobes **5** and **6**.

emission, and therefore compromising the sensitivity in more complex biological environments.

As a solution to these problems, we grafted two water-soluble hydroxycoumarin dyes by CuAAC to a glucopyranoside ring (Fig. 3).^{37–39} While the glycoprobes formed could be used for selective Ag(I) detection in aqueous solution (80% water), we observed that the addition of the coumarin groups to the different ring positions of a glucopyranoside resulted in a different sensing behaviour.^{37,39} Whereas the introduction of coumarin to the C3,4-positions of glucoside led to fluorescence quenching of the probe upon interaction with Ag(I) (**5**), the addition of the dyes to the C2,3-positions led to a fluorescence enhancement after chelation with Ag(I) (**6**). This was reasoned to be due to the formation of different binding motifs between Ag(I) and the glycoprobes: whereas **5** binds to Ag(I) in a 1:1 stoichiometry, **6** chelates the ion in a 2:1 stoichiometry, thereby resulting in the chelation-enhanced fluorescence (CHEF).³⁹ The fluorescence “turn-on” glycoprobe **6** has also proven suitable for imaging intracellular Ag(I) ions in a human hepatoma cell line. This study suggests that the substitution of fluorophores at different positions of the sugar ring may enable the modulation of the sensing mechanism of the glycoprobe synthesized.

Glycoprobes for targeted imaging of intracellular species

Having developed sugar-ring modified glycoprobes, we set out to install fluorophore-receptor motifs to the anomeric carbon of sugars. These glycoprobes with fully available sugar-ring hydroxy groups possess (1) enhanced water solubility allowing the full-aqueous sensing of analytes and (2) targeting ability for cell-membrane sugar receptors. Therefore, taking on board these two points, we synthesized a series of galactosyl probes for ASGPr-targeted cell imaging.

A bis-triazolyl rhodamine probe appended with two galactosyl groups, using CuAAC coupling of 1-azido-1-deoxy-galactose with a bis-*O*-propynyl rhodamine B, was prepared. The glycoprobe **7** displays a “turn-on” fluorescence upon selective binding with Hg(II) because of the spiro-lactam-ring-opening mechanism of rhodamine (Fig. 4).⁴⁰ Owing to the presence of the galactosyl moieties, **7** was shown to detect Hg(II) selectively in 100% water solution by fluorescence spectroscopy. More interestingly, the probe displayed an ability to selectively image intracellular Hg(II) in Hep-G2 with a high ASGPr expression level, rather than control cells, HeLa (human cervical cell line) and HCT-116



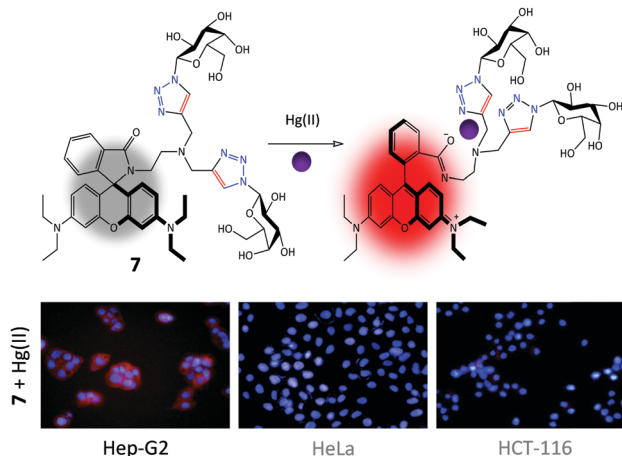


Fig. 4 Structure and the Hg(II)-chelation mode of galactorhodamine probe **7** and its targeted fluorescence imaging of intracellular Hg(II) in Hep-G2 (human hepatoma) cells over HeLa (human cervical cancer cell line) and HCT-116 (human colon cancer cell line). Reproduced with permission from ref. 40 (*Chem. Commun.*, 2014, **50**, 11735). Copyright: The Royal Society of Chemistry.

(human colon cell line), with minimal ASGPr expression (Fig. 4) (the expression level of ASGPr in these cells were evaluated using the polymerase chain reaction). In contrast, a polyethylene glycol (instead of galactose) analogue showed unselective imaging of Hg(II) for all the cell lines used.⁴¹ We also observed that the knockdown of ASGPr in Hep-G2 and preincubation of Hep-G2 with excess D-galactose largely diminished the fluorescence intensity observed. These observations suggest that the targeted intracellular Hg(II) imaging by the glycoprobe was dependent on a specific galactose–ASGPr interaction.

Subsequently, we set out to expand the scope of galactosyl probes for ASGPr-targeted imaging of other analytes. Using a known reaction-based hydrogen disulfide (H₂S) probe **8'** (the azide group quenches the fluorescence of the naphthalimide *via* intramolecular charge transfer, thus, reduction to an amine by H₂S results in a fluorescence “turn-on” response),⁴² we prepared the galactonaphthalimide probe **8** (Fig. 5).⁴³ By using a panel of different cells preincubated with H₂S, we determined that the glycoprobe displayed a Hep-G2-selective imaging ability, whereas the fluorescence of **8'**^{44,45} was much weaker in all the cell types used. This was because of the high ASGPr expression level in Hep-G2 over the control cells. Also, suppression of ASGPr in Hep-G2 and a galactose-competition assay both decreased the fluorescence intensity of the glycoprobe. This probe provides a useful means for the fluorogenic detection of hepatocellular H₂S, an important gaseous transmitter produced in the liver.

Since Zn(II) is an important physiological ion and is also implicated in many pathological processes such as Alzheimer's diseases,⁴⁶ we glycosylated a smart Zn(II) probe previously developed by Xu, Yoon and co-workers.⁴⁷ The “click” addition of the galactosyl moiety to the probe⁴⁸ was performed to improve (1) the water solubility thereby achieving full-aqueous sensing of the ion, (2) the working pH range and (3) the targeting ability for Hep-G2 with high ASGPr expression. For the third point, likewise, while the control probe (**9'**) was able to illuminate Zn(II) in all the cell lines used,

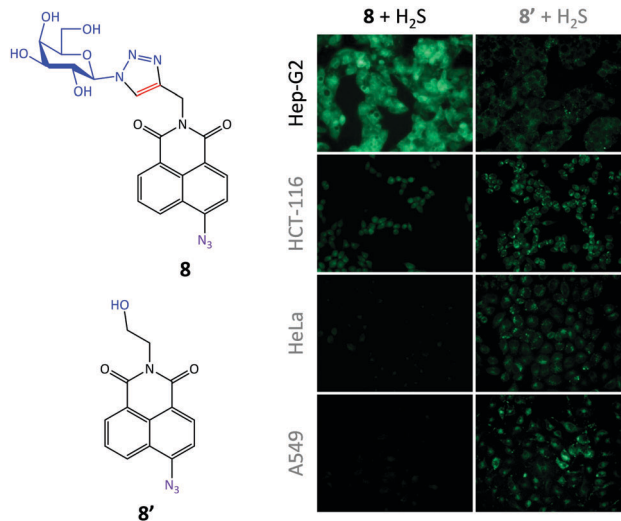


Fig. 5 Structure of galactonaphthalimide (**8**) and control (**8'**) probes and their targeted fluorescence imaging of intracellular H₂S in Hep-G2 (human hepatoma) cells over HCT-116 (human colon cancer cell line), HeLa (human cervical cancer cell line) and A549 (human lung cancer cell line). Reproduced with permission from ref. 43 (*Chem. Commun.*, 2015, **51**, 3653). Copyright: The Royal Society of Chemistry.

the galactoprobe **9** displayed an enhanced ability to selectively image the ion only in Hep-G2 cells (Fig. 6), mediated by the selective ASGPr–galactose interaction. Most notably, the presence of the glycosyl group also reduced the cytotoxicity of the control probe (naphthalimide structures are known to be toxic to cells), providing some insight into the potential development of glycosyl drugs.

These previous investigations corroborate our belief that the addition of a glycosyl targeting agent to an organic-dye based fluorescent probe can increase the selective internalization by a specific cell that highly expresses the glycoligand receptor. In the meanwhile, the water solubility and other sensing properties

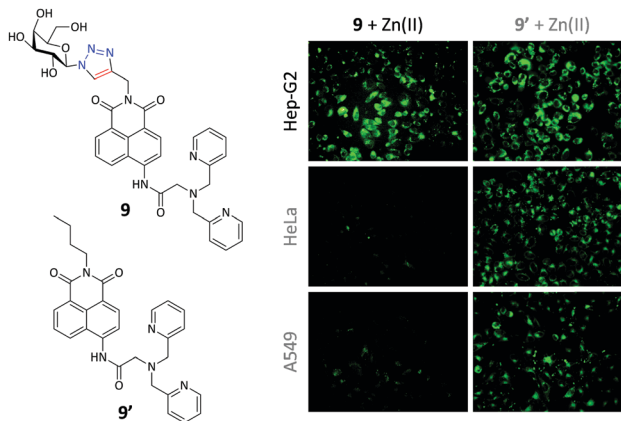


Fig. 6 Structure of galactonaphthalimide (**9**) and control (**9'**) probes and their targeted fluorescence imaging of intracellular Zn(II) in Hep-G2 (human hepatoma) cells over HeLa (human cervical cancer cell line) and A549 (human lung cancer cell line). Reproduced with permission from ref. 48 (*Chem. Commun.*, 2015, **51**, 11852). Copyright: The Royal Society of Chemistry.



such as pH working range can also be improved by this strategy. In a very recent study we also determined that a galactonaphthalimide pH probe could be used to selectively accumulate and fluoresce in lysosome (with acidic pH) of Hep-G2,⁴⁹ since ASGPr is responsible for trafficking exogenous ligands to lysosome for degradation. This suggests the possibility of targeted lysosome localization in a cell that expresses a sugar receptor.

Glycophores for lectin sensing

Lectins are sugar-recognition proteins widely identified in plants, microorganisms and mammalian cells.⁵⁰ As a class of promising biomarkers for disease diagnosis (such as for bacteria and cancer cell detection), a number of elegant lectin probes have been synthesized. For more information on this topic readers are directed to a recent comprehensive review written by the Vidal group.⁵¹ We began this project following our interest in the construction of macrocyclic glycoconjugates.⁵² A pyrenyl β -cyclodextrin (pyrene-CD) was synthesized by CuAAC of seven pyrene alkynes to azido β -CD (Fig. 7).⁵³ We subsequently determined that the pyrene-CD could

form supramolecular ensembles with two glycorhodamine probes (the GalNAc-probe **10** and GlcNAc-probe **11**, where GalNAc and GlcNAc are *N*-acetyl-galactosamine and *N*-acetyl-glucosamine, respectively). The fluorescence of the probes was quenched probably through the static quenching between intimately stacked pyrene cluster and rhodamine. Subsequently, the addition of a selective lectin (soybean agglutinin for GalNAc and wheat germ agglutinin for GlcNAc) resulted in the concentration-dependent fluorescence recovery of the construct, over a panel of unselective proteins. With this research we demonstrated a unique CD-based supramolecular, fluorogenic lectin probe whose hydrophobic CD cavity can be further modified for targeted drug delivery.⁵⁴

Aggregation-induced-emission (AIE) describes the emission enhancement of fluorogens caused by aggregation as a result of changes in the microenvironment.^{55,56} Restriction in rotation (RIR) and restriction in vibration (RIV) are two typical mechanistic explanations for AIE, amongst others.⁵⁶ Recently, vibration-induced-emission (VIE), which is a very interesting and exceptional photophysical property, where a single molecule can emit two different light colours with large Stokes shift upon tuning the planarity of phenazine derivatives, was described by Tian and co-workers.^{57–59}

Since lectins can aggregate multivalent glycophores, we synthesized two divalent glyco-diketopyrrolopyrrole (DPP) probes for lectin detection (in cooperation with Hua's group) (Fig. 8).⁶⁰ The glycophores **12** (mannosyl) and **13** (galactosyl) with DPP of typical AIE property showed sharp fluorescence enhancement in the presence of a mannosose-selective lectin (concanavalin A – Con A) and galactose-selective lectin (peanut agglutinin – PNA), rather than unselective lectins, proteins and ions. Scanning electron microscopic analysis suggested that the incubation of a selective lectin with the AIE-glycophore led to the formation of small aggregates, thereby rationalizing the observed fluorescence enhancements.

We also demonstrated that the direct supramolecular assembly between glycophores and unmodified AIEgens is amenable to lectin sensing. Silole is an archetypical AIEgen used for biosensing (Fig. 9).⁶¹ The AIEgen can form emissive nanoparticles in aqueous solution. As a consequence, we used two red-emitting glyco-DCM (dicyanomethylene-4*H*-pyran) probes to form supramolecular assemblies with the silole particle by hydrophobic interactions between the two dyes. While the DCM moiety can stack to the surface of silole-based particles, the hydrophilic glycoligands are exposed to the solution for lectin recognition. The assemblies formed showed a red fluorescence upon excitation of the cyan AIEgen because of the Förster Resonance Energy Transfer (FRET) from silole to glyco-DCM. Subsequently, the addition of selective lectins resulted in recovery of the silole fluorescence as a result of the removal of the glycophores from the AIE particle, thereby enabling a ratiometric method for lectin analyses. This ratiometric rationale (shift in emission color), which is different from conventional AIE-based fluorimetric sensing (increase/decrease in emission intensity), which might improve the sensitivity and accuracy of lectin detection using AIEgens.



Fig. 7 Structure of glycorhodamine probes **10** and **11** for supramolecular assembly with pyrenyl β -cyclodextrin (pyrene-CD).



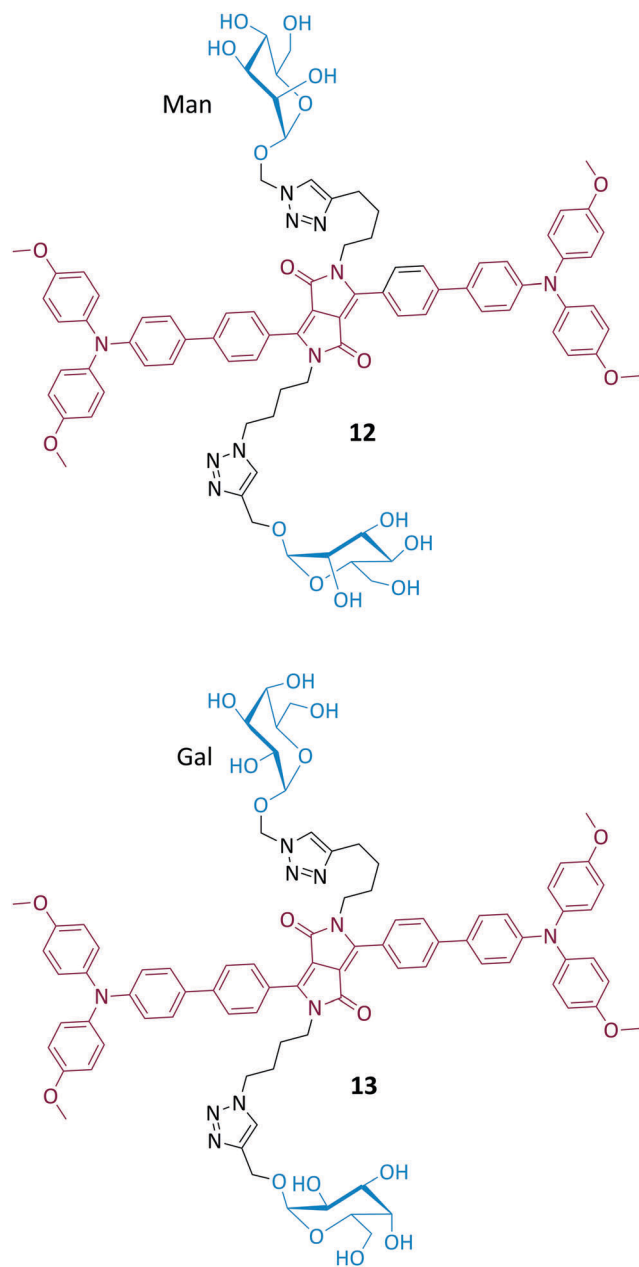


Fig. 8 Structure of glyco-diketopyrrolopyrrole probes **12** and **13** for fluorogenic lectin detection by aggregation-induced-emission.

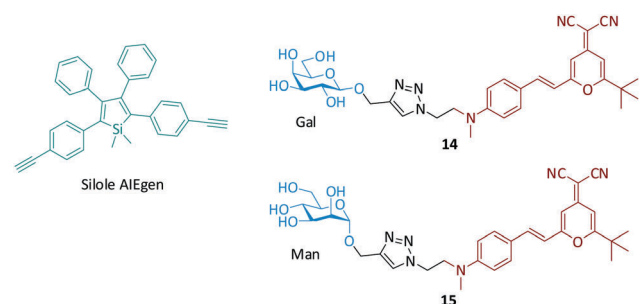


Fig. 9 Structure of the silole AIEgen and glyco-DCM (dicyanomethylene-4H-pyran) probes for the fluorogenic detection of lectins.

Fluorogenic glycoprobe-2D material composites for targeted imaging and theranostics

Because of their outstanding optical, electronic and mechanical properties, low-dimensional materials (such as carbon nanotube, graphene and graphene analogues) have received tremendous interest for the development of functional materials and devices. In the low-dimensional material family 2D graphene represents the most important material for a diverse range of applications.^{62–65} Graphene oxide (GO) which possesses better water solubility and biocompatibility than pristine graphene has also been widely employed in biomedical applications.^{66–68} Our approach for constructing self-assembled glycoprobe-GO composites depends on the fluorescence quenching ability of GO (to enable a simple “turn-on” detection protocol)^{66–68} and the large surface area of the material to cluster the glycoligands for enhanced binding with lectins and cell-surface receptors.

We initiated our investigations by carrying out the self-assembly between the GalNAc-rhodamine probe **10** and GO by π -stacking and electrostatic interaction (Fig. 10).⁶⁹ Using atomic force microscopy and other spectroscopic techniques we determined that the glycoprobe can conjugate with GO to form a 2D “glycosheet” with quenched fluorescence. The fluorescence quenching was determined to be caused by FRET between the fluorophore and GO with a large absorbance band.⁶⁶ With this fluorogenic material in hand, we determined that the presence of SBA (GalNAc-selective lectin) over other non-selective proteins increased the fluorescence of the system in a concentration-dependent manner. The subsequent cellular assay indicated that the 2D glycosheet could image Hep-G2 cells with ASGPr expression. However, the change of the GalNAc targeting agent to GlcNAc (glycoprobe **11**) as well as knockdown of ASGPr in Hep-G2 cells compromised the imaging ability. This



Fig. 10 Schematic illustration of the glycorhodamine probe assembled 2D graphene oxide (GO) glycosheet for targeted cell imaging.



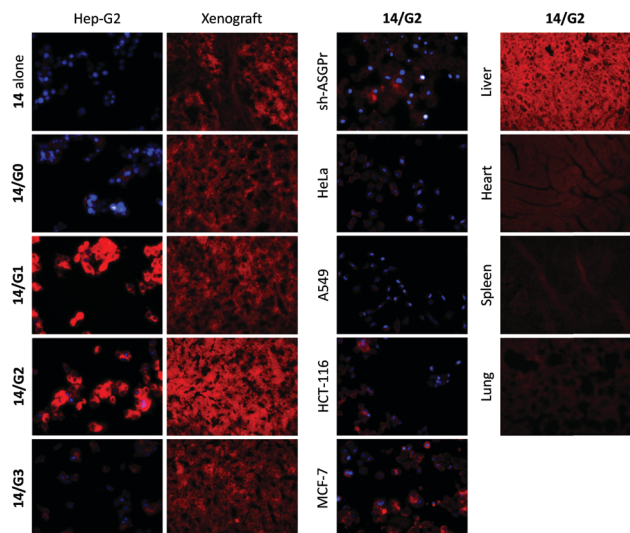


Fig. 11 Graphene oxide (**G0**: 0–10 nm; **G1**: 50–200 nm; **G2**: 200–500 nm; **G3**: 500–1000 nm) size dependent selective imaging of cells and tissues using glycoprobe **14** based 2D glycosheets. Reproduced with permission from ref. 72 (*J. Mater. Chem. B*, 2015, **3**, 9182). Copyright: The Royal Society of Chemistry.

research paves the way for targeted imaging using glycoprobe-assembled 2D materials. In a subsequent study we also demonstrated that the GO platform could accommodate two types of glycoligands grafted with two fluorophores and different emission wavelengths for the simultaneous investigation of two sugar–lectin interactions, in a homogeneous solution.⁷⁰

Having established our first generation of 2D glycosheet probes, we then set out to optimize the size of the GO material substrate. We first determined that, of the four GOs with different size distributions used (0–10 nm, 50–200 nm, 200–500 nm and 500–1000 nm), the material with a moderate size had the best sensitivity for lectins.⁷¹ In a subsequent study we further observed the GO size effect for imaging cells.⁷² We determined that the imaging ability of glyco-DCM probe (**14**, see Fig. 11) based GO 2D glycosheet composite for Hep-G2 was dependent on the size of the material substrate. The moderate-sized GO (200–500 nm) produced the best imaging effect, over other GOs (Fig. 11). Notably, the fluorescence intensity of this glycosheet composite with Hep-G2 was much stronger than that of the glycoprobe alone, suggesting that the presence of GO may enhance the targeted imaging ability of small-molecular glycoprobes. We also observed this size-effect with Hep-G2 xenograft tissue; the imaging was shown to be selective for ASGPr-expressing cells and tissues (xenograft and liver since ASGPr is predominantly expressed on hepatocytes) over other control samples. More importantly, we also demonstrated that, besides the glycoprobe an anticancer drug can also be co-loaded onto the GO platform, resulting in targeted theranostics (imaging combined with drug delivery), as illustrated in Fig. 12.⁷² The 2D glycosheet (**14**/GO) co-loaded with hydroxycamptothecin exhibited both imaging fluorescence and cytotoxicity predominantly for Hep-G2 over HeLa and A549.

In a recent study, we also demonstrated that this glycosheet composite strategy was applicable for a graphene analogue, 2D



Fig. 12 Schematic illustration of glycoprobe–GO composite material for targeted theranostics (combined imaging and drug delivery). Reproduced with permission from ref. 72 (*J. Mater. Chem. B*, 2015, **3**, 9182). Copyright: The Royal Society of Chemistry.

molybdenum disulphide (MoS_2).⁷³ The 2D glycosheets from MoS_2 displayed targeted imaging for Hep-G2 over control cells. Interestingly, the endocytosed 2D MoS_2 sheets could also release toxic levels of reactive oxygen species (ROS) to kill the cancer cell upon light irradiation. In contrast, a much lower ROS concentration, and thus toxicity was observed for control cells with minimal ASGPr expression. This research suggests that a broader range of 2D materials for glycoprobe assembly is possible and the potential of using this tactic for targeted photodynamic disease therapy. In comparison with GO, we also determined that the 2D MoS_2 had a better working concentration range in improving the ASGPr-targeting imaging of Hep-G2 cells with glycoprobe **14**, suggesting that 2D materials with a similar morphology but different chemical components might function differently at the cellular interface.⁷⁴ In addition to 2D materials, we also proved the potential of using conjugated polymers (in cooperation with Tan's group) as a material substrate to form supramolecular ensembles with glycoprobes. Similarly, these material composites displayed the ability to selectively sense lectins,⁷⁵ and image Hep-G2 cells in a targeted manner.⁷⁶

Summary and perspective

We have highlighted recent progress towards the development of glycoprobes for sensing, imaging and theranostics. The applications of these glycoprobes range from the solution based ion/lectin detection to targeted cell imaging and theranostics. The glycoprobes are readily synthesized using the CuAAC click chemistry between a variety of sugars and fluorophores. Glycosylation of conventional organic-dye based probes has proven to be effective in (1) improving the water solubility for aqueous analyses, (2) lowering the toxicity of some organic dyes and, in particular (3) imparting the probes with a targeted imaging and theranostic ability.

Having demonstrated the general merits and scope of the glycoprobe tactic, our ongoing research interests are focusing on the following targets.



(1) Structural diversification of the sugar targeting agent for different types of cells. The identification of more complex glycan structures as targeting group for cell-surface receptors would be required for improving the targeting ability of glyco probes since monosaccharides might not avoid unselective internalization by cells.

(2) Extension of the glycoprobe strategy for the detection of pathogens such as viruses and bacteria that significantly express specific lectins.⁷⁷

(3) Optimization of the 2D glycosheet composite materials by adjusting the glycoprobe structure for more efficient assembly with 2D materials. The structural unification for 2D materials is also important to achieve good reproducibility. Meanwhile, changing the substrate to other low-dimension materials (such as the zero-dimensional gold nanoparticle^{78–80} and one-dimensional carbon nanotubes) could be carried out in order to construct even more material composites for targeted diagnosis and theranostics.

(4) Finally the *in vivo* imaging and theranostics using glycoprobes and their material composites will be an important goal to achieve.

Acknowledgements

We warmly thank our collaborators and students who have contributed significantly to the papers featured in this article. Professor He Tian from ECUST is thanked for his tremendous support of our research. This research is supported by the 973 project (2013CB733700), the Science and Technology Commission of Shanghai Municipality (15540723800), the National Natural Science Foundation of China (21572058, 21576088) and the Shanghai Rising-Star Program (16QA1401400) (X.-P. H.). The Catalysis And Sensing for our Environment (CASE) network is thanked for research exchange opportunities. T. D. J. and J. X. thank ECUST for guest professorships.

Notes and references

- For a recent themed issue, see: C. J. Chang, T. Gunnlaugsson and T. D. James, *Chem. Soc. Rev.*, 2015, **44**, 4484–4486.
- For a recent themed issue, see: C. J. Chang, T. Gunnlaugsson and T. D. James, *Chem. Soc. Rev.*, 2015, **44**, 4176–4178.
- C. R. Bertozzi and L. L. Kiessling, *Science*, 2001, **291**, 2357–2364.
- T. Feizi and W. Chai, *Nat. Rev. Mol. Cell Biol.*, 2004, **5**, 582–588.
- G. W. Hart and R. J. Copeland, *Cell*, 2010, **143**, 672–676.
- F.-T. Liu and G. A. Rabinovich, *Nat. Rev. Cancer*, 2005, **5**, 29–41.
- J. Mukherjee, H. J. de Haas, A. D. Petrov, A. Tawakol, N. Haider, A. Tahara, C. C. Constantinescu, J. Zhou, H. H. Boersma, T. Imaizumi, M. Nakano, A. Finn, Z. Fayad, R. Virmani, V. Fuster, L. Bosca and J. Narula, *J. Nat. Med.*, 2014, **20**, 215–219.
- L. L. Kiessling and R. A. Splain, *Annu. Rev. Biochem.*, 2010, **79**, 619–653.
- J. B. Burgess, J. U. Baenziger and W. R. Brown, *Hepatology*, 1992, **15**, 702–706.
- T. Lawrence and G. Natoli, *Nat. Rev. Immunol.*, 2011, **11**, 750–761.
- R. Xu, R. P. de Vries, X. Zhu, C. M. Nycholat, R. McBribe, W. Yu, J. C. Paulson and I. A. Wilson, *Science*, 2013, **342**, 1230–1235.
- E. I. Rigopoulou, D. Roggenbuck, D. S. Smyk, C. Liaskos, M. G. Mythilinaiou, E. Feist, K. Conrad and D. P. Bogdanos, *Autoimmunity Rev.*, 2012, **12**, 260–269.
- K. Jain, P. Kesharwani, U. Gupta and N. K. Jain, *Biomaterials*, 2012, **33**, 4166–4186.

- X.-P. He, J. Xie, Y. Tang, J. Li and G.-R. Chen, *Curr. Med. Chem.*, 2012, **19**, 2399–2405.
- X.-P. He, Y.-L. Zeng, Y. Zang, J. Li, R. A. Field and G.-R. Chen, *Carbohydr. Res.*, 2016, **429**, 1–22.
- H. Yuasa, N. Miyagawa, T. Izumi, M. Nakatani, M. Izumi and H. Hashimoto, *Org. Lett.*, 2004, **6**, 1489–1492.
- H. Yuasa, N. Miyagawa, M. Nakatani, M. Izumi and H. Hashimoto, *Org. Biomol. Chem.*, 2004, **2**, 3548–3556.
- Y.-K. Yang, S. Shim and J. Tae, *Chem. Commun.*, 2010, **46**, 7766–7768.
- Y.-C. Hsieh, J.-L. Chir, H.-H. Wu, P.-S. Chang and A.-T. Wu, *Carbohydr. Res.*, 2009, **344**, 2236–2239.
- J. Xie, M. Ménand, S. Maisonneuve and R. Méthivier, *J. Org. Chem.*, 2007, **72**, 5980–5985.
- N. K. Singhal, B. Ramanujam, V. Mariappanadar and C. P. Rao, *Org. Lett.*, 2006, **8**, 3525–3528.
- Y.-C. Hsieh, J.-L. Chir, H.-H. Wu, C.-Q. Guo and A.-T. Wu, *Tetrahedron Lett.*, 2010, **51**, 109–111.
- B. Ke, W. Chen, N. Ni, Y. Cheng, C. Dai, H. Dinh and B. Wang, *Chem. Commun.*, 2013, **49**, 2494–2496.
- Y.-B. Chen, Y.-J. Wang, Y.-J. Lin, C.-H. Hu, S.-J. Chen, J.-L. Chir and A.-T. Wu, *Carbohydr. Res.*, 2010, **345**, 956–959.
- K.-H. Chen, C.-Y. Lu, H.-J. Cheng, S.-J. Chen, C.-H. Hu and A.-T. Wu, *Carbohydr. Res.*, 2010, **345**, 2557–2561.
- Y.-C. Hsieh, J.-L. Chir, S.-T. Yang, S.-J. Chen, C.-H. Hu and A.-T. Wu, *Carbohydr. Res.*, 2011, **346**, 978–981.
- S. Ou, Z. Lin, C. Duan, H. Zhang and Z. Bai, *Chem. Commun.*, 2006, 4392–4394.
- A. Mitra, A. K. Mittal and C. P. Rao, *Chem. Commun.*, 2011, **47**, 2565–2567.
- Y.-B. Ruan, H. Yi and J. Xie, *Photochem. Photobiol. Sci.*, 2013, **12**, 1103–1109.
- Y. Mikata, A. Ugai, K. Yasuda, S. Itami, S. Tamotsu, H. Konno and S. Iwatsuki, *Chem. Biodiversity*, 2012, **9**, 2064–2075.
- L. Garcia, S. Maisonneuve, J. Xie, R. Guillot, P. Dorlet, E. Rivière, M. Desmadril, F. Lambert and C. Policar, *Inorg. Chem.*, 2010, **49**, 7282–7288.
- L. Garcia, S. Maisonneuve, J. O.-S. Marcu, R. Guillot, F. Lambert, J. Xie and C. Policar, *Inorg. Chem.*, 2011, **50**, 11352–11362.
- L. Garcia, M. Lazzaretti, A. Diguët, F. Mussi, F. Bisceglie, J. Xie, G. Pelosi, A. Buschini, D. Baigl and C. Policar, *New J. Chem.*, 2013, **37**, 3030–3034.
- Z. Song, X.-P. He, C. Li, L.-X. Gao, Z.-X. Wang, Y. Tang, J. Xie, J. Li and G.-R. Chen, *Carbohydr. Res.*, 2011, **346**, 140–145.
- Z. Song, X.-P. He, X.-P. Jin, L.-X. Gao, L. Sheng, Y.-B. Zhou, J. Li and G.-R. Chen, *Tetrahedron Lett.*, 2011, **52**, 894–898.
- X.-P. He, X. Juan, G. Chen and K. Chen, *Chin. J. Chem.*, 2012, **30**, 2874–2878.
- X.-P. He, Z. Song, Z.-Z. Wang, X.-X. Shi, K. Chen and G.-R. Chen, *Tetrahedron*, 2011, **67**, 3343–3347.
- J.-L. Xue, X.-P. He, J.-W. Yang, D.-T. Shi, C.-Y. Cheng, J. Xie, G.-R. Chen and K. Chen, *Carbohydr. Res.*, 2012, **363**, 38–42.
- D.-T. Shi, X.-L. Wei, Y. Sheng, Y. Zang, X.-P. He, J. Xie, G. Liu, Y. Tang, J. Li and G.-R. Chen, *Sci. Rep.*, 2014, **4**, 4252.
- K.-B. Li, Y. Zang, H. Wang, J. Li, G.-R. Chen, T. D. James, X.-P. He and H. Tian, *Chem. Commun.*, 2014, **50**, 11735–11737.
- K.-B. Li, H. Wang, Y. Zang, X.-P. He, J. Li, G.-R. Chen and H. Tian, *ACS Appl. Mater. Interfaces*, 2014, **6**, 19600–19605.
- F. Yu, X. Han and L. Chen, *Chem. Commun.*, 2013, **49**, 12234–12249.
- D.-T. Shi, D. Zhou, Y. Zang, J. Li, G.-R. Chen, T. D. James, X.-P. He and H. Tian, *Chem. Commun.*, 2015, **51**, 3653–3655.
- C. Yu, X. Li, F. Zeng, F. Zheng and S. Wu, *Chem. Commun.*, 2013, **49**, 403–405.
- L. A. Montoya and M. D. Pluth, *Chem. Commun.*, 2012, **48**, 4767–4769.
- Z. Xu, J. Yoon and D. R. Spring, *Chem. Soc. Rev.*, 2010, **39**, 1996–2006.
- Z. Xu, K.-H. Baek, H. N. Kim, J. Cui, X. Qian, D. R. Spring, I. Shin and J. Yoon, *J. Am. Chem. Soc.*, 2010, **132**, 601–610.
- L. Dong, Y. Zang, D. Zhou, X.-P. He, G.-R. Chen, T. D. James and J. Li, *Chem. Commun.*, 2015, **51**, 11852–11855.
- Y. Fu, J. Zhang, H. Wang, J.-L. Chen, P. Zhao, G.-R. Chen and X.-P. He, *Dyes Pigm.*, 2016, **133**, 372–379.
- H. Lis and N. Sharon, *Chem. Rev.*, 1998, **98**, 637–674.
- S. Cecioni, A. Imberty and S. Vidal, *Chem. Rev.*, 2015, **115**, 525–561.
- J. Xie and N. Bogliotti, *Chem. Rev.*, 2014, **144**, 7678–7739.



- 53 X.-P. He, R.-H. Li, S. Maisonneuve, Y. Ruan, G.-R. Chen and J. Xie, *Chem. Commun.*, 2014, **50**, 14141–14144.
- 54 Y. Chen and Y. Liu, *Chem. Soc. Rev.*, 2010, **39**, 495–505.
- 55 J. Luo, Z. Xie, W. Y. Lam, L. Cheng, H. Chen, C. Qiu, H. S. Kwok, X. Zhan, Y. Liu, D. Zhu and B. Z. Tang, *Chem. Commun.*, 2001, 1740–1741.
- 56 J. Mei, N. L. C. Leung, R. T. K. Kwok, J. W. Y. Lam and B. Z. Tang, *Chem. Rev.*, 2015, **115**, 11718–11940.
- 57 W. Huang, L. Sun, Z. Zheng, J. Su and H. Tian, *Chem. Commun.*, 2015, **51**, 4462–4464.
- 58 Z. Zhang, Y.-S. Wu, K.-C. Tang, C.-L. Chen, J.-W. Ho, J. Su, H. Tian and P.-T. Chou, *J. Am. Chem. Soc.*, 2015, **137**, 8509–8520.
- 59 H. Wang, Z. Zhang, H. Zhou, T. Wang, J. Su, X. Tong and H. Tian, *Chem. Commun.*, 2016, **52**, 5459–5462.
- 60 Y. Hang, X.-P. He, L. Yang and J. Hua, *Biosens. Bioelectron.*, 2015, **65**, 420–426.
- 61 J.-D. Zhang, J. Mei, X.-L. Hu, X.-P. He and H. Tian, *Small*, 2016, DOI: 10.1002/smll.201601470.
- 62 A. K. Geim and K. S. Novoselov, *Nat. Mater.*, 2009, **6**, 183–191.
- 63 A. K. Geim, *Science*, 2009, **324**, 1530.
- 64 K. S. Novoselov, A. K. Geim, S. V. Morozov, D. Jiang, Y. Zhang, S. V. Dubonos, I. V. Grigorieva and A. A. Firsov, *Science*, 2004, **306**, 666–669.
- 65 K. P. Loh, Q. Bao, G. Eda and M. Chhowalla, *Nat. Chem.*, 2010, **2**, 1015–1024.
- 66 E. Morales-Narváez and A. Merkoçi, *Adv. Mater.*, 2012, **24**, 3298–3308.
- 67 L. Feng, L. Wu and X. Qu, *Adv. Mater.*, 2013, **25**, 168–186.
- 68 X.-P. He, Y. Zang, T. D. James, J. Li and G.-R. Chen, *Chem. Soc. Rev.*, 2015, **44**, 4239–4248.
- 69 H.-L. Zhang, X.-L. Wei, Y. Zang, J.-Y. Cao, S. Liu, X.-P. He, Q. Chen, Y.-T. Long, J. Li, G.-R. Chen and K. Chen, *Adv. Mater.*, 2013, **25**, 4097–4101.
- 70 D.-K. Ji, G.-R. Chen, X.-P. He and H. Tian, *Adv. Funct. Mater.*, 2015, **25**, 3483–3487.
- 71 D.-L. Ji, Y. Zhang, X.-P. He and G.-R. Chen, *J. Mater. Chem. B*, 2015, **3**, 6656–6661.
- 72 D.-L. Ji, Y. Zhang, Y. Zang, W. Liu, X. Zhang, J. Li, G.-R. Chen, T. D. James and X.-P. He, *J. Mater. Chem. B*, 2015, **3**, 9182–9185.
- 73 D.-K. Ji, Y. Zhang, Y. Zang, J. Li, G.-R. Chen, X.-P. He and H. Tian, *Adv. Mater.*, 2016, DOI: 10.1002/adma.201602748.
- 74 D. Xie, D.-K. Ji, Y. Zhang, J. Cao, H. Zheng, L. Liu, Y. Zang, J. Li, G.-R. Chen, T. D. James and X.-P. He, *Chem. Commun.*, 2016, **52**, 9418–9421.
- 75 W.-T. Dou, Y.-L. Zeng, Y. Lv, J. Wu, X.-P. He, G.-R. Chen and C. Tan, *ACS Appl. Mater. Interfaces*, 2016, **8**, 13601–13606.
- 76 W.-T. Dou, Y. Zhang, Y. Lv, J. Wu, Y. Zang, C. Tan, J. Li, G.-R. Chen and X.-P. He, *Chem. Commun.*, 2016, **52**, 3821–3824.
- 77 X.-P. He, Y.-L. Zeng, X.-Y. Tang, N. Li, D.-M. Zhou, G.-R. Chen and H. Tian, *Angew. Chem., Int. Ed.*, 2016, DOI: 10.1002/anie.201606488.
- 78 X.-L. Hu, H.-Y. Jin, X.-P. He, T. D. James, G.-R. Chen and Y.-T. Long, *ACS Appl. Mater. Interfaces*, 2015, **7**, 1874–1878.
- 79 X.-P. He, X.-L. Hu, H.-Y. Jin, J. Gan, H. Zhu, J. Li, Y.-T. Long and H. Tian, *Anal. Chem.*, 2015, **87**, 9078–9083.
- 80 X.-L. Hu, Y. Zang, J. Li, G.-R. Chen, T. D. James, X.-P. He and H. Tian, *Chem. Sci.*, 2016, **7**, 4004–4008.

